8th International Conference
on
Wind Turbine Noise
Lisbon – 12th to 14th June 2019

Simulation of sound radiation of wind turbines using large-scale finite element models

Thomas Grätsch, Marc Zarnekow, Frank Ihlenburg
Hamburg University of Applied Sciences
thomas.graetsch@haw-hamburg.de

Summary

In this paper the development of a vibro-acoustic finite element model at large scale is presented that can be used for structural-borne and air-borne path analysis in order to identify the critical path of sound propagation within a wind turbine. The investigation is focused on the transfer of mechanical vibrations from the gear box through the drivetrain. It is shown that a simplified numerical-analytical model of gear vibrations leads to mechanical resonance peaks that correspond to tonalities in measured far-field sound spectra.

1. Introduction

The control of noise emissions from wind turbines has become an issue of growing attention and strict regulation over the last decades where tonalities in the far-field spectrum are of particular importance. These far-field tonalities can be traced back to mechanical vibration sources within the drivetrain like the gear box or the generator. Measurements show that tonalities in the far field sound (pressure) spectra correspond with meshing frequencies of the gear box high speed stage.

The focus in this research is the simulation of transfer paths from vibrational sources (e.g. the gear box or generator) to radiating components of the turbines (e.g. blades or nacelle cover) with the goal to identify critical transfer paths within the turbine and further to find efficient design measures to reduce the radiation of tonal noise. In our study a 2.5 MW wind turbine of our project partner at operational state is considered.

The paper is organized as follows: In Section 2 a hybrid numerical-analytical approach is presented for modeling the excitation sources at the gears which combines a series of detailed finite element analyses for different meshing configurations of helical gears with analytical models for the transient gear dynamics. In Section 3 a large-scale finite element model of the whole wind turbine is developed which includes all major parts like the drivetrain, the mainframe, the nacelle, the blades and the tower in sufficient fine mesh resolution. In this model the calculated excitations as described in Section 2 are used as input data to represent

the operating load spectra. The focus in this section is on the analysis of structure-borne transfer paths. Further, some brief considerations regarding accuracy, convergence and solution efficiency of the finite element model are made. Based on the dynamic response of structural parts, in Section 4 the model is also used to assess the radiation of air-borne sound where analytical methods are employed for calculating the frequency spectrum in the far-field in order to identify the critical tonalities. Section 5 shows a first example of application of the new developed model.

2. Numerical-Analytical Analysis of Gear Excitation

Gear vibrations due to varying mesh stiffness are a major source of tonal noise radiated from wind turbines. In order to obtain realistic excitations at operational state, in this section a hybrid numerical-analytical model of the gear dynamics is presented that combines a series of detailed finite element analysis of meshing configurations with analytical models for the transient dynamics of helical gears.

2.1 Finite Element Modelling of Meshing Stiffness

In a first step, the angle-dependent mesh stiffness of the gears is obtained from a sequence of static FE analyses that cover a complete meshing cycle. In this approach, the geometry of meshing gears can be modelled in a desired level of detailing including arbitrary geometric properties of interest such as helical angles, profile shift, or shape errors. The finite element model uses contact analysis in the area of potential contact between the gear flanks. A prerequisite for obtaining a stable and accurate solution is that the finite element resolution is sufficiently fine. Fig. 1 shows a section of a typical finite element model of a helical gearing.

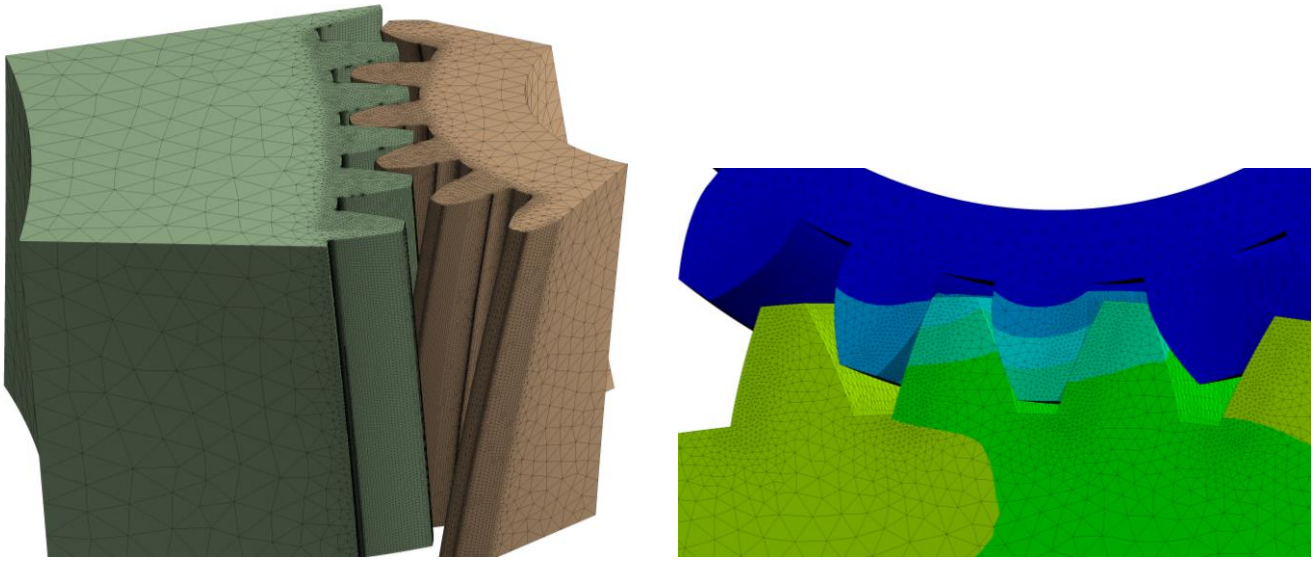

Fig. 1: Finite element model of a helical gearing

Our approach is validated with results from the literature, which shows excellent agreement for spur gears [1], see Fig. 2, while helical gears have not yet been extensively studied in the literature. For the considered spur gear connection, our results seem even more realistic than reported since the meshing stiffness changes rapidly as it should be in a realistic meshing configuration when a double tooth contact suddenly changes into a single tooth contact.

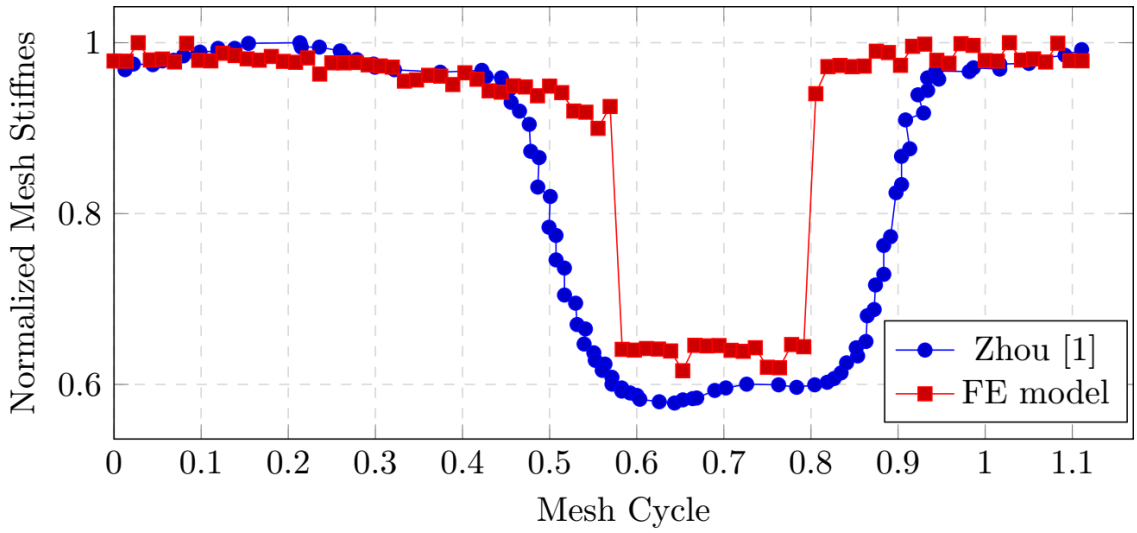

Fig. 2: Validation of mesh stiffness for spur connection, [1]

After having validated our approach, the procedure is applied to our actually considered wind turbine. Fig. 3 shows the results of a meshing stiffness analysis for a typical helical gearing.

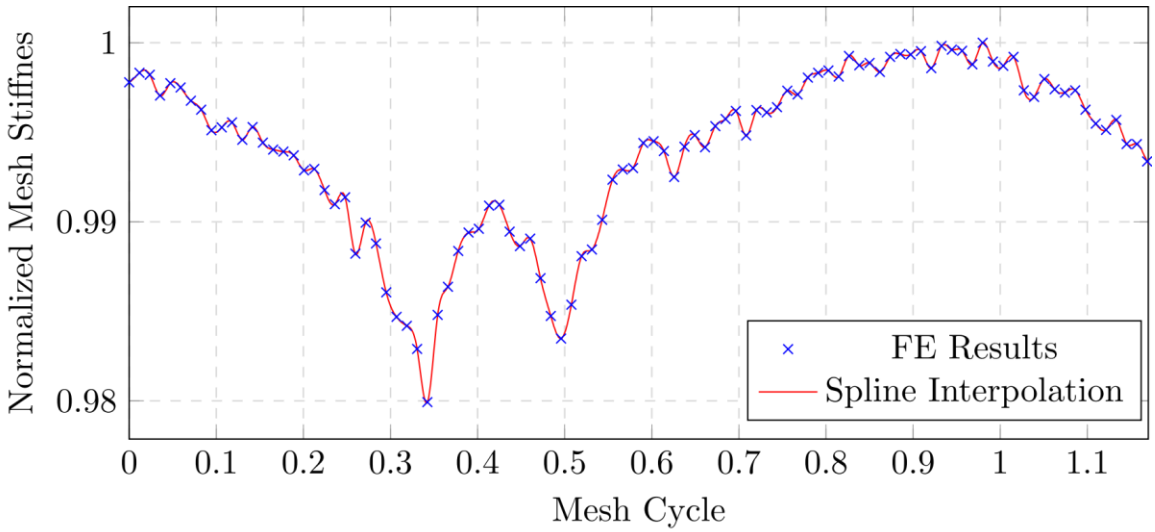

Fig. 3: Varying mesh stiffness as for a helical gear connection

2.2 Analytical Model of Gear Dynamics

The dynamic interaction within a gear pairing is simulated using a two-body model, see [2], with four degrees of freedom as shown in Fig. 4. The bodies are coupled via a linear spring-damper with a time-dependent spring constant $k_m(t)$ that is obtained from Fig. 3. The model also includes the stiffness and the damping of the gear support structure (e.g. bearing, shaft etc.).

Replacing the rotational degree of freedom by the transmission error (TE), the analytical model consists of three degrees of freedom which are the transmission error and the radial gear displacements along the line-of-action. The system is subject to parametric excitation by the time-varying stiffness $k_m(t)$ and to forced excitation by an error function e(t) that can be used to include the effect of fabrication errors or wear.

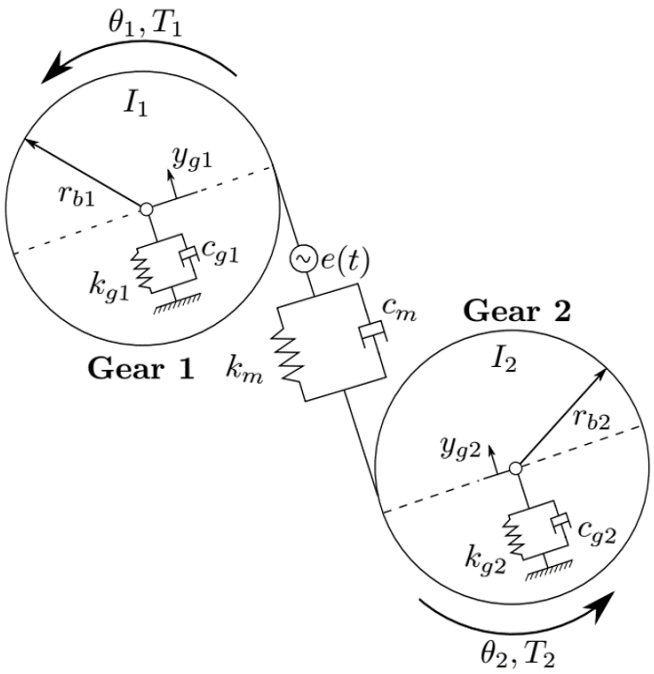

Fig. 4: Analytical model of gear dynamics

The resulting analytical model is a system of ordinary differential equations of second order which can be numerically solved in time with standard methods such as the Runge-Kutta scheme:

$$m_1\ddot{y}_{g1} + c_{g1}\dot{y}_{g1} - c_m\left(\dot{x} - \dot{y}_{g1} + \dot{y}_{g2}\right) + k_{g1}y_{g1} - k_m\left(x - y_{g1}{+}_{g2}\right) = -c_m\dot{e} - k_m e$$

$$m_2\ddot{y}_{g2} + c_{g2}\dot{y}_{g2} + c_m\left(\dot{x} - \dot{y}_{g1} + \dot{y}_{g2}\right) + k_{g2}y_{g2} + k_m\left(x - y_{g1}{+}_{g2}\right) = c_m\dot{e} + k_m e$$

$$m_e\ddot{x} + c_m\left(\dot{x} - \dot{y}_{g1} + \dot{y}_{g2}\right) + k_m\left(x - y_{g1}{+}_{g2}\right) = c_m\dot{e} + k_m e - m_e W_0\left(\frac{r_{b1}^2}{I_{g1}} - \frac{r_{b2}^2}{I_g 2}\right)$$

The stiffness parameter $k_m(t)$ is obtained from the above mentioned finite element analysis of the gear meshing. The solution of the system of differential equations is obtained in the time domain and can be transformed into the frequency domain by a Fast Fourier Transformation, see Fig. 5.

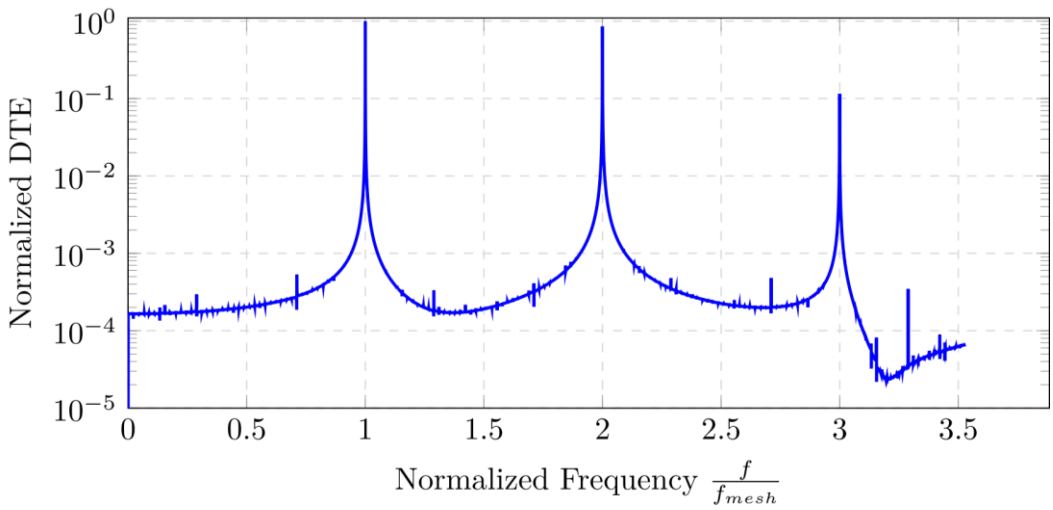

Fig. 5: Frequency spectrum of the transmission error

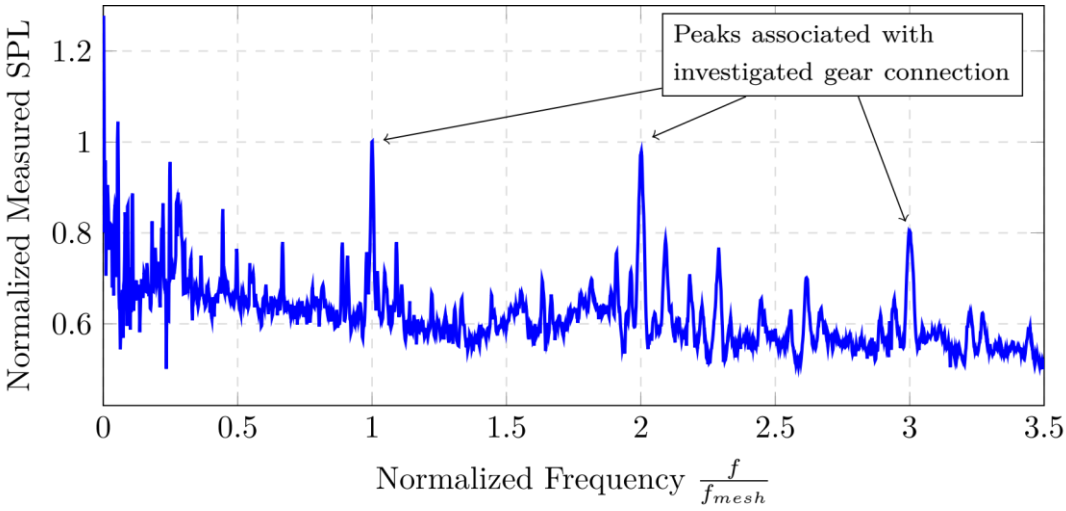

Fig. 6: Measured sound frequency spectrum of wind turbine gear box on a test-rig

To evaluate the results of the gear excitation spare modelling, the calculated excitation spectrum is compared with a sound pressure level spectrum measured on a gearbox test-rig. As can be seen from Fig. 6, the calculated transmission error frequency spectrum is in sound qualitative agreement with frequency response graphs of sound radiation, obtained from acoustic measurements on the gearbox test rig. Over an analysis spectrum of several KHz, the gearbox associated peak frequencies in both spectra agree very good and the relation of the peaks in the calculated excitation spectrum correspond well with the relation of the measured ones.

Critical tonalities in the sound spectrum of wind turbines are mainly caused by mechanical components in the drive train, for example the meshing gears. In Fig. 7 it can be seen that in the far-field sound spectrum of the wind turbine characteristic peaks occur at the same frequencies as calculated with the gear excitation model or as seen in the gear test rig measurement. Therefore, there is a need to investigate the transfer path of sound propagation within the turbine.

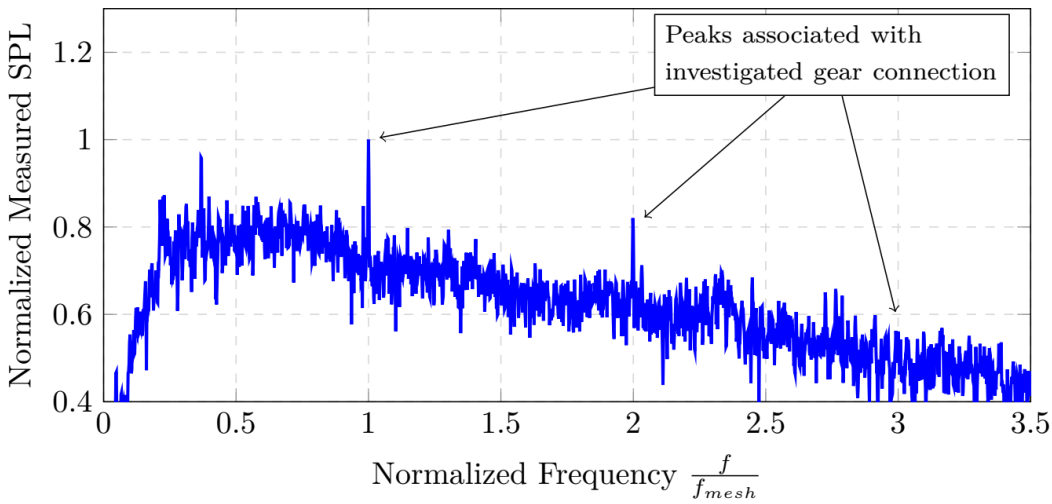

Fig. 7: Measured far-field sound spectrum of wind turbine gear box on a test-rig

The model for large-scale transfer path analysis is discussed in the next section, where either the transmission error as a displacement excitation or a force excitation at the bearings of the gear box can be applied as input, where both input data are directly obtained as a solution of the above given system of differential equations.

3. Development of Large-Scale Finite Element Model

For identifying the structure-borne transfer path of sound propagation a large scale finite element model of the whole wind turbine is developed. The finite element model consists of more than 10 million degrees of freedom and is solved in a broad-frequency range.

3.1 Finite Element Modelling

The finite element model includes all major parts like the drivetrain, the mainframe, the nacelle cover, the blades and the tower. The overall wind turbine model is modeled bottom-up, that means, at first, each component is modeled separately. The main steps for this component-wise modeling include the CAD generation and/ or import, the identification of relevant parts for the transfer analysis, defeaturing of local disturbances that are not necessary to resolve in the finite element model, and meshing of each component.

The large-scale finite element model is eventually built using the single components. As a part of the full model Fig. 8 shows the finite element model of the drivetrain when mounted on the mainframe.

The main modeling steps of this assembling step are the adequate definition of the interfaces between the components. Interfaces, where negligibly small deformations are assumed, are modeled as rigid connections, as for example between the main shaft and the shrink disc of the planet carrier or at the massive connection between main bearing and main frame. For other interfaces between components, such as bearings, mount or similar connections, stiffness and damping matrices are employed at the interfaces, which account for the related stiffness and damping of the connection. To obtain the 6x6 stiffness matrices in these cases, the nominal load at the operating point is applied in all 6 degrees of freedom in space to obtain the corresponding stiffness as the derivation of the force-displacement curve of the respective bearing or other connecting elements.

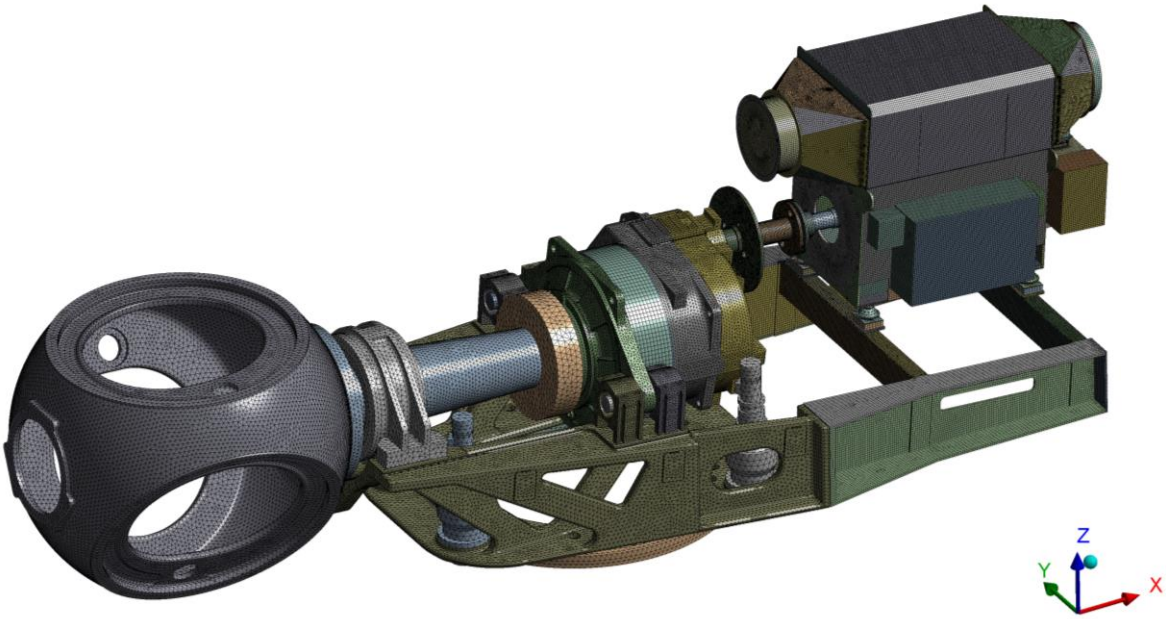

Fig. 8: Finite element model of the drivetrain mounted on mainframe

3.2 Mesh Density Evaluation

A crucial question in finite element analysis is whether the results are accurate and reliable. In order to assure that the discretization error at the component level is sufficiently small - hence that the solution quality of the computation is high - some considerations have been made:

For each single component several mesh density analyses are performed to evaluate the mesh quality. First of all, convergence curves of major local output quantities are calculated. Next, the model assurance criterion (MAC-value) is used to compare different finite element meshes with each other, where the reference solution is a so-called overkill solution with an extreme fine mesh resolution. All modes up to 1.5 times the highest frequency of interest for the vibro-acoustic simulation are compared. Further, in the same manner, the frequency response assurance criterion (FRAC-value) is employed to ensure the convergence in the frequency response up to the highest frequency of interest. Fig. 9 and 10 show the MAC- respective FRAC-values of the main frame before and after having found the sufficient fine mesh resolution.

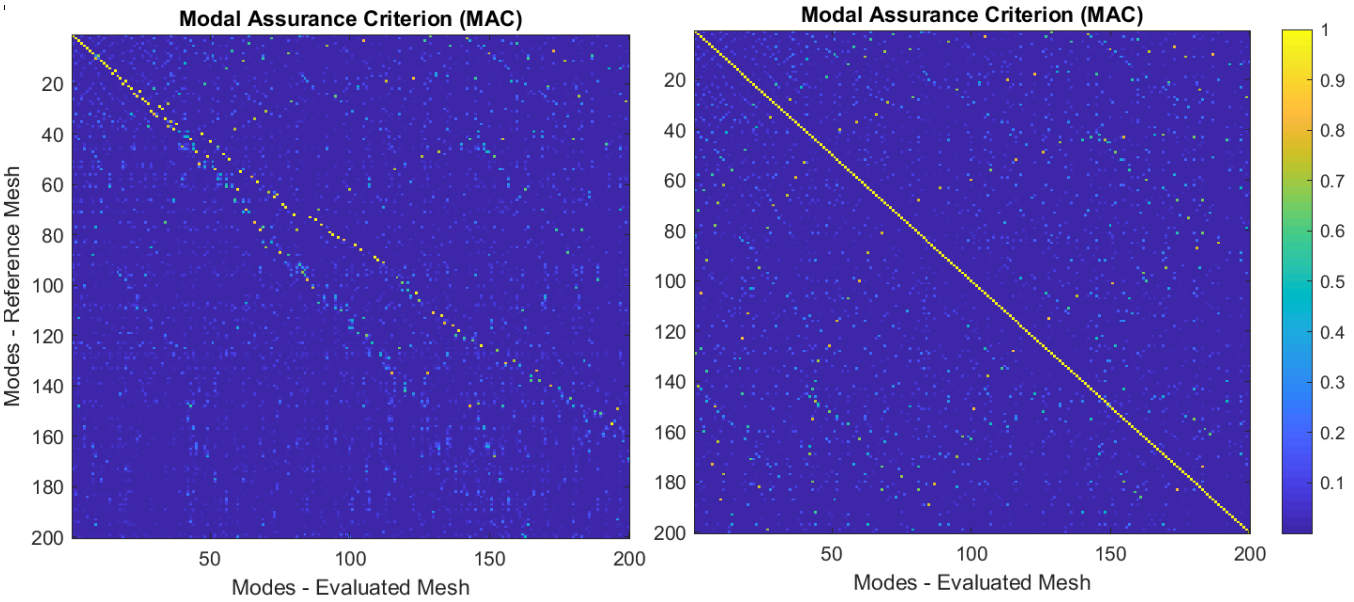

Fig. 9: MAC-values of a coarse mesh (left) and a sufficiently fine mesh (right)

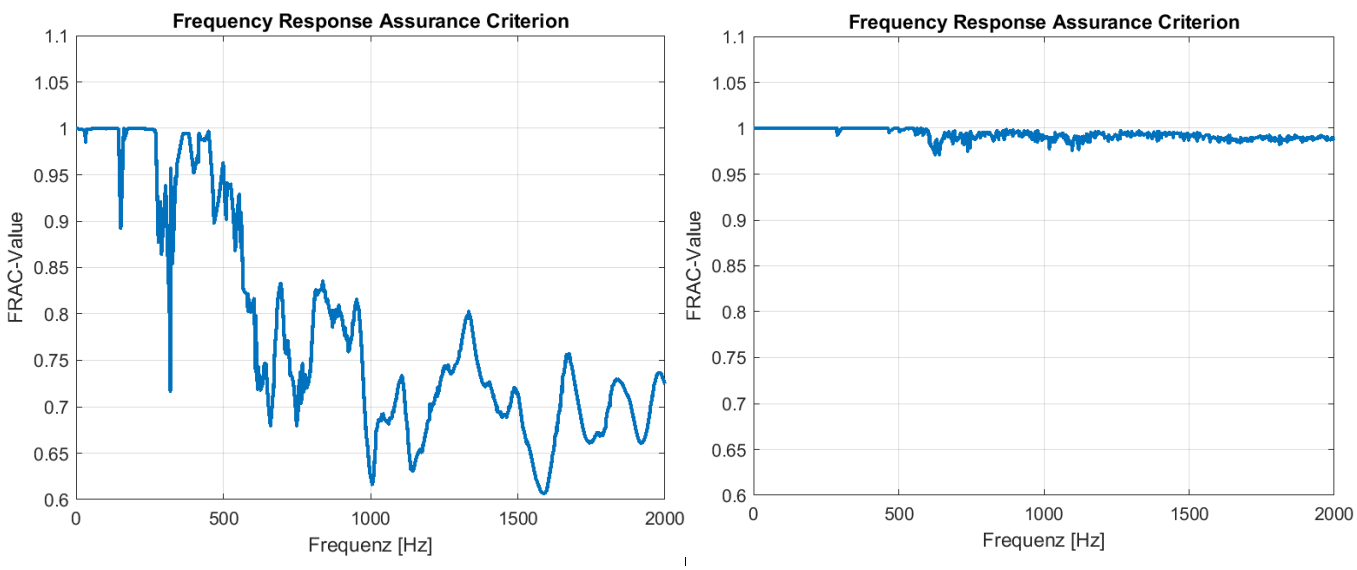

Fig. 10: FRAQ-values of a coarse mesh (left) and a sufficiently fine mesh (right)

3.3 Calculating Dynamic Transfer Functions

In order to find the critical transfer path, a frequency response analysis is conducted where a unit excitation is applied at the potential excitation source that accounts for the excitations during operation. In doing so, the transfer function is obtained which is equal to the frequency response at every desired location of the full model for every result quantity of interest. In order to obtain the response under operating conditions the linear behaviour of a frequency response analysis is exploited according to the linear equation

$$x(f) = T(f) \cdot TE(f)$$

where $x(f)$ denotes the frequency response at operation conditions, $T(f)$ denotes the transfer function obtained as described above by applying a unit excitation and $TE(f)$ denotes the operational excitation such as the transmission error at the gear box bearing according to Fig. 5. This procedure can be applied at the same time for all relevant excitation sources, and due to the linearity of the analysis, a superposition can be carried out to obtain the overall response or to evaluate the different contributions of the single excitation sources.

In addition to the displacement frequency response some advanced structural output quantities can be calculated in this approach such as velocities, energies or the ERP level of certain parts of the structure. As an example, Fig. 11 shows the displacement response of the nacelle cover at a critical frequency of 566.5 Hz when excited by the transmission error at the gear box bearing. The corresponding ERP level is shown in Fig. 12 for certain panels of interest. This results can now be used to identify critical panels and to suggest design changes to reduce the peaks.

To deal with the computational effort of the full model, standard model reduction methods of structural dynamics like the component mode synthesis method are employed. When applying these methods it can be shown for the considered wind turbine that the computational effort for solving the full system can be reduced by 90% in both computing time and memory allocation while the resulting error is negligibly small that is less than 1% in the considered frequencies for all modes up to 2000 Hz.

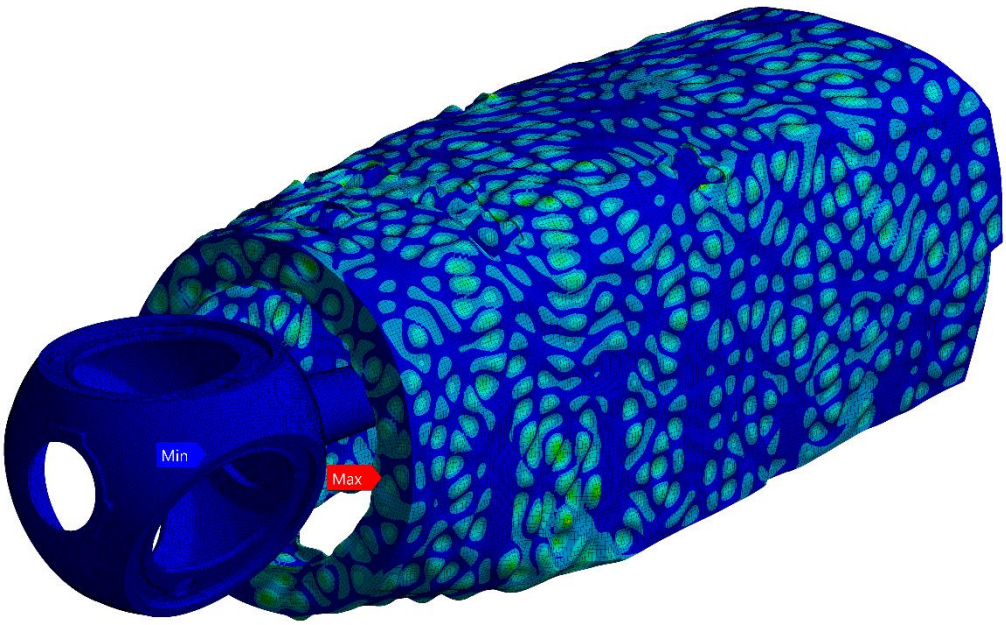

Fig. 11: Frequency response of the nacelle cover at 566.5 Hz due to gear excitation

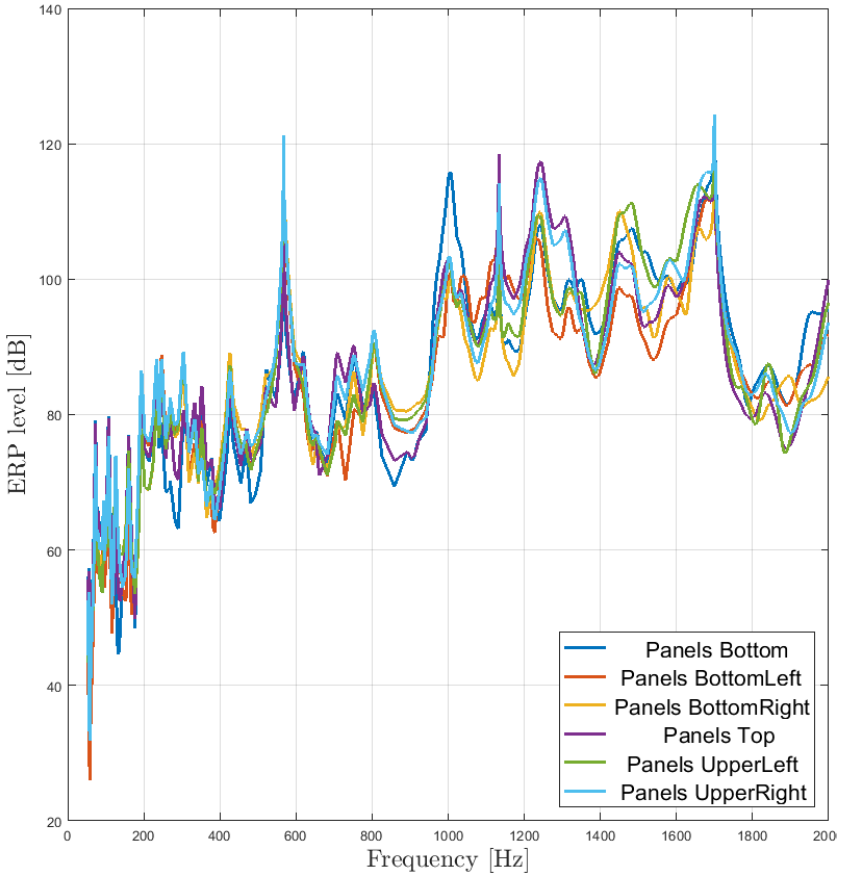

Fig. 12: ERP level of different panels of the nacelle cover from 0 to 2000 Hz due to gear excitation

4. Air-Borne Transfer Path Analysis

Dynamic structural results like the ERP level can provide useful results in the evaluation of the sound radiation behaviour of structures. But since simplifications and assumptions are made here, e.g. an ideal radiation efficiency is assumed and dynamic properties of cavities are not considered, their application can be limited under certain circumstances. Therefore, some additional air-borne transfer path analysis is necessary.

To investigate the air-borne transfer path, the full-scale finite element model can also be used for acoustic simulations. In this regard, the acoustic domain within the nacelle is modelled with acoustic finite elements. In this approach, the acoustic fluid field is coupled with the structural field, which is commonly referred to as fluid-structure interaction (FSI). FSI can generally be modelled via two different approaches, either as fully coupled (two-way coupling) or weakly coupled (one-way coupling).

The fully coupled formulation defines a mutual interaction of structure and fluid fields over both kinematic and kinetic coupling conditions at the interface and is commonly described by the following formulation, see [3]:

$$\left(-\omega^2 \begin{bmatrix} M_s & 0 \\ \rho_0 R^T & M_f \end{bmatrix} + j\omega \begin{bmatrix} C_s & 0 \\ 0 & C_f \end{bmatrix} + \begin{bmatrix} K_s & -R \\ 0 & K_f \end{bmatrix}\right) \begin{Bmatrix} u_s \\ p_f \end{Bmatrix} = \begin{Bmatrix} f_s \\ f_f \end{Bmatrix}$$

In this coupled problem the acoustic domain is interacting with the structural part, which is the nacelle cover. Spacial displacement and pressure degrees of freedom are employed in the coupled analysis, where the number per element depends on the actual type of the finite element used.

The weak FSI-coupling defines only a kinematic coupling condition at the interface by assuming that the acoustic fluid field does not influence the structure. Therefore, the structure part is solved independently, and subsequently the so-obtained structural vibrations are applied to the acoustic fluid as boundary conditions. The weak coupling is computationally more efficient, but it is, of course, a more simplified approach than the full coupling.

The described acoustic simulations can be used to investigate the acoustic transfer inside the nacelle, see Fig. 13 (left), where the pressure distribution due to vibrating nacelle cover panels is shown. Based on the results of the acoustic simulation, further acoustic finite element models are used to evaluate the sound radiation into the far field due to the vibrating panels, see Fig. 13 (right).

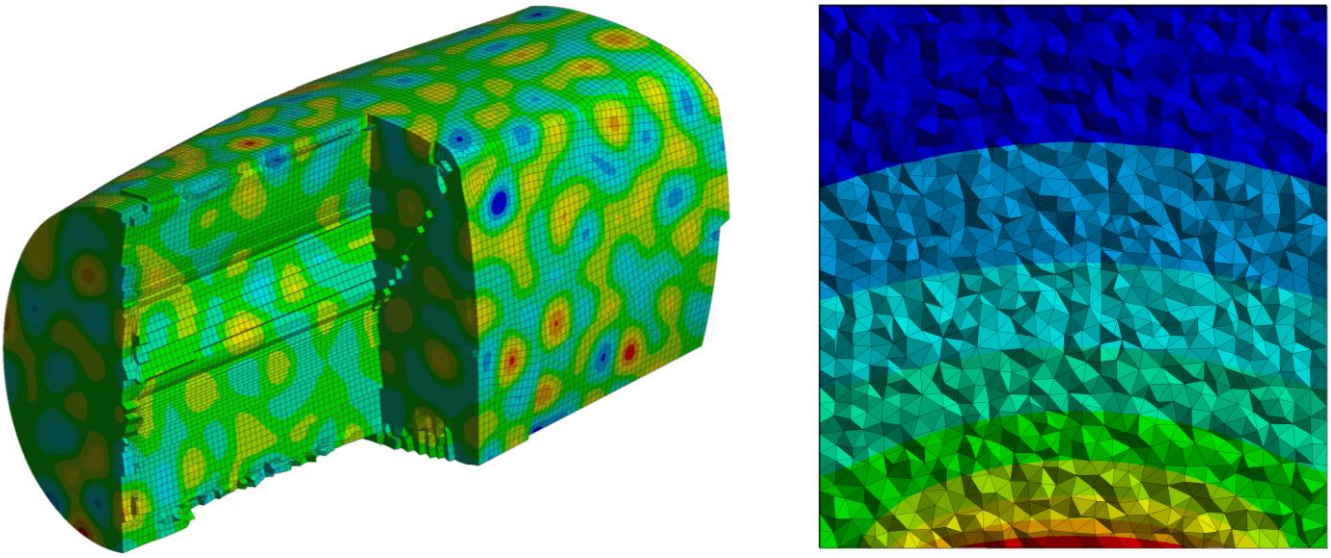

Fig. 13: Pressure distribution within nacelle due to weakly coupling to vibrating panels (left) and a section of an acoustic simulation of radiation into the far-field (right)

5. Computational Example

As an application of the presented approach a computational example is considered. The model consists of the whole drivetrain as shown in Fig. 8 including the nacelle cover. The finite element model consists of 2.5 Million nodes yielding 7.5 Million degrees of freedom. The CMS method is used for model reduction.

The goal in this principal scenario is to identify the critical transfer path between a known (vibrational) source and a receiver. As investigated excitation source in this case, the transmission error of the high speed gear stage is applied at the meshing gears. The aim is to evaluate how much and via which paths this gear vibration are radiated by the nacelle cover. Therefore the received quantity is described by the equivalent radiated power of the nacelle cover panels. That means for simplification reasons the acoustic radiation is approximated by the ERP.

There are basically three potential transfer paths to transport the sound from the vibration source (high speed gear stage) to the receiver (nacelle cover). The three possible transfer paths are through the torque arm (TA), through the main bearing (MB), or via the generator (GEN), see the three coloured lines in Fig. 14. As an additional aspect of this theoretical computational example, the transfer path via the generator is bridged by a rigid connection directly to the main frame. It is expected, that by applying this modification and its direct and stiff connection to the receiver, an artificially dominant and critical transfer path is established.

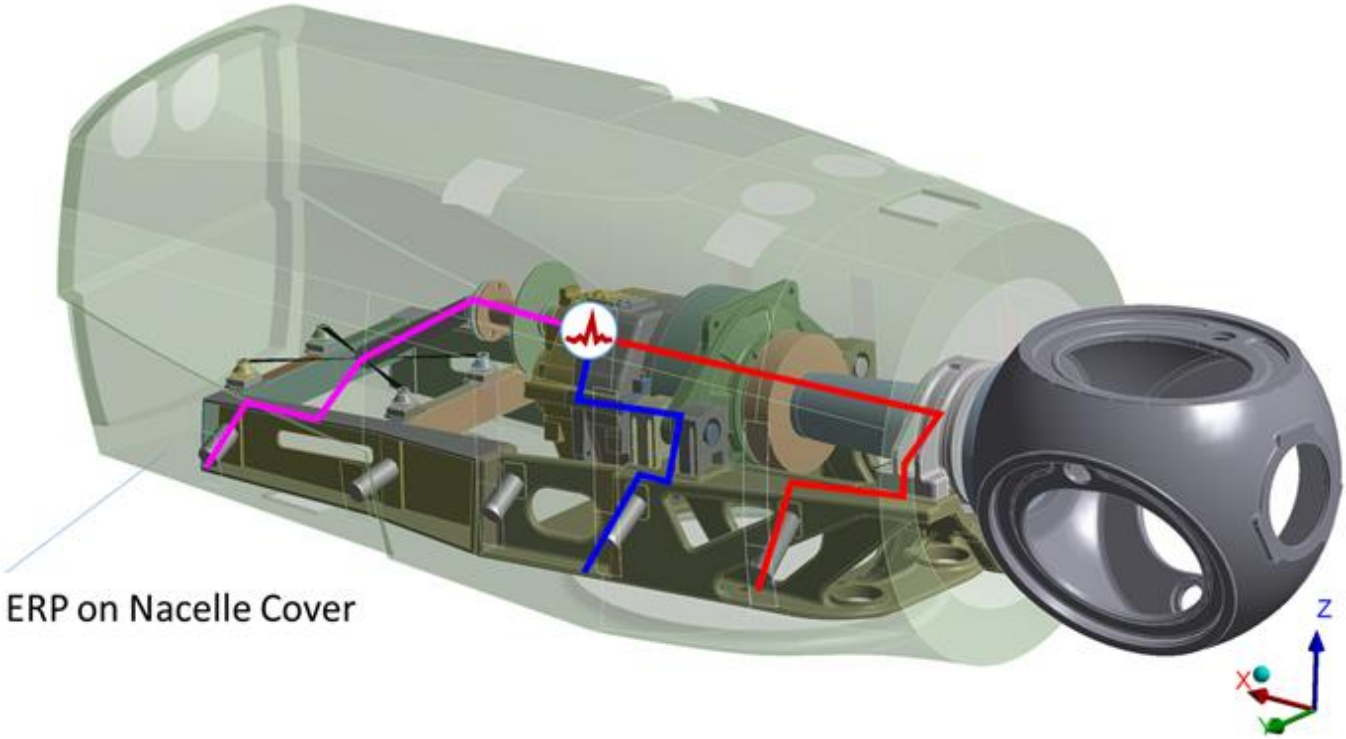

Fig. 14: Three possible transfer paths from gear excitation (source) to nacelle cover (receiver)

In order to find the critical path, the idea is to isolate one of the paths from the other by cutting the other two paths in the finite element model, respectively. For this, the assumption is made that the influence and the interaction between the three paths on the global dynamic behavior is negligibly small. This assumption can be confirmed by superposing the ERP response of the three individual paths and comparing this curve with the ERP response obtained by a full model analysis including all the three paths. Fig. 15 shows the calculated ERP level of the nacelle cover and compares the results of the reference model with all paths combined and the superposition of the ERP levels of the isolated contribution of the single transfer paths. Therefore it can be confirmed, that the modeling for this approach has an negligible small influence on the ERP levels.

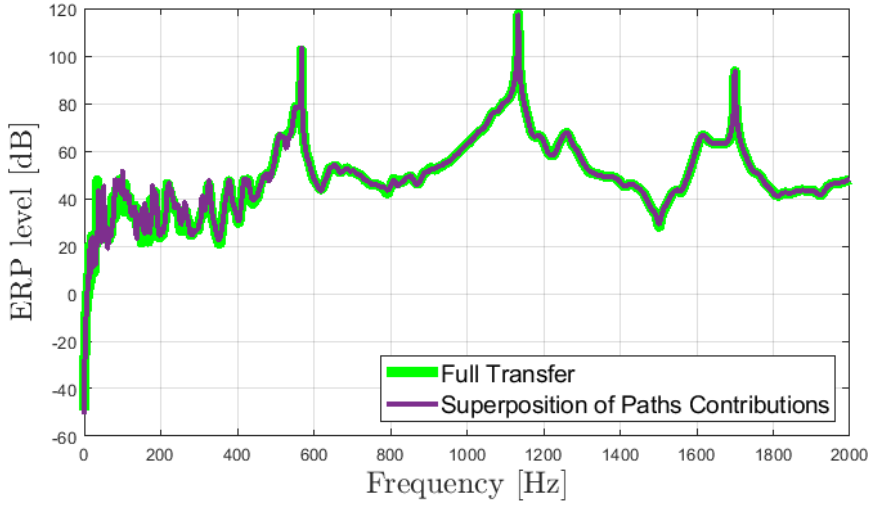

Fig. 15: Validation of modeling approach of isolating the path contributions

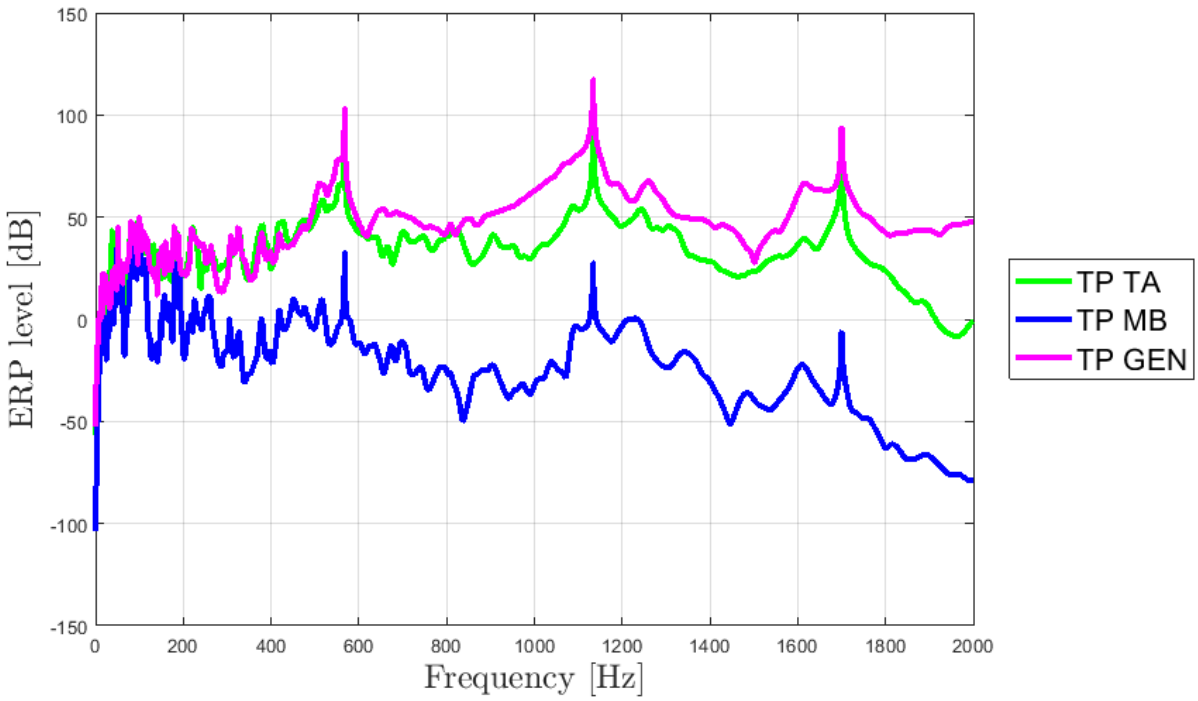

Fig. 16: ERP level of nacelle cover depending on transfer paths via torque arm (TA), main bearing (MB) or generator (GEN)

Fig. 16 shows the contributions of the three different transfer paths. As it can be seen the transfer path along the generator dominates nearly the complete frequency range while the transfer path via the torque arm is less dominant and the contributions by transfer path via the main bearing are negligible small at frequencies above 200 Hz.

Therefore the obtained results confirm the initial assumption that the modified bridged generator path represents a dominating and critical transfer path in this example scenario. The results show that the modelling approach provides the ability to evaluate the contributions of different transfer paths and therefore to identify critical vibration and sound transmission.

The identification of such critical transfer paths through the described modelling approach can be used to identify constructive problems and improvement measures. However, it must be added that absolute statements for a real turbine are not possible at this point, because the

generator is not fully resolved. Hence, when using a more detailed generator model, this transfer path might be less dominant. However, this computational example shows how the presented approach can be employed in general in order to identify the critical transfer path of sound propagation.

6. Conclusions

In this paper, a finite element modelling approach to simulate the vibro-acoustic transfer path behaviour of a wind turbine under operating conditions has been presented.

The excitation spectrum of a gear stage is calculated by an hybrid analytical-numerical approach combining detailed static finite element with analytical gear dynamics. This approach is verified on a spur gear connection and then extended to a helical gear connection of a wind turbine gearbox. The gear dynamic modelling provides the frequency spectrum of the gear excitation under operating conditions, which has been compared to an measured sound pressure spectrum.

The structure-borne transfer paths of the considered wind turbine are investigated using a dynamic large-scale finite element model. Further, the aspects of mesh density evaluation and model reduction techniques are discussed. The dynamic large-scale finite element model is used to calculate transfer functions for all relevant quantities of interest. Subsequently, the transfer functions are combined with the previously determined load spectra to obtain the behaviour under operating conditions.

In addition to the structure-borne transfer path, the air-borne transfer path is addressed with different acoustic finite element modelling approaches that are used to investigate the acoustic behaviour of cavities (e.g. inside the nacelle) or to investigate the radiation of vibrating panels (e.g. nacelle cover, blades, or tower) .

A computational example of large scale finite element analysis shows how the contributions from several transfer paths can be evaluated separately in order to show how the presented approach can be employed in general in order to identify the critical transfer path of propagation.

References

[1] Zhou, J and Wenlei, S (2014) *Vibration and Noise Radiation Characteristics of Gear Transmission System* Jnl Low Frequency Noise, Vibration and Active Control 30(4), 485-502

[2] Özgüven, H and Houser, D (1988) *Dynamic analysis of high speed gears by using loaded static transmission error* Jnl of Sound and Vibration 125 (1), 71-83

[3] Sandberg, G, Davidsson, P and Wernberg, P (2009) *Fundamentals of Fluid-Structure Interaction* In: Computational Aspects of Structural Acoustics and Vibration, 23-101